A new piezoelectric fatigue testing machine in pure torsion for ultrasonic gigacycle fatigue tests: application to forged and extruded titanium alloys

A. NIKITIN[1], C. BATHIAS[1] and T. PALIN-LUC[2]

[1]*University Paris Ouest Nanterre La Defense, LEME, 50, rue de Sevres, Ville-d'Avray, 92410, France,* [2]*Arts et Metiers Paris Tech, I2M, CNRS, Universite de Bordeaux, Esplanade des Arts et Metiers, Talence 33405, France*

Received Date: 27 February 2015; Accepted Date: 25 June 2015; Published Online: 2015

ABSTRACT This article briefly discusses the history of the development of ultrasonic fatigue testing methods, with respect to industrial needs. The development of ultrasonic techniques and the progress made in the computer industry have led to improvements in ultrasonic testing techniques. It has been shown, that existing ultrasonic testing systems have limitations that lead to the need for a new ultrasonic fatigue testing machine operating in pure torsion. This paper introduces the development of a new piezoelectric machine working in the continuous regime (i.e. without pulse-pause). This machine has been used to investigate the Very High Cycle Fatigue (VHCF) properties of the VT3-1 alpha beta aeronautical titanium alloy (which is similar to Ti–6Al–4V) produced by two manufacturing processes: forging and extrusion. The extruded titanium alloy has a higher VHCF strength in torsion compared to the forged one. Despite the maximum shear stress occurring at the specimen surface under torsion loading, internal fatigue crack initiation can be observed in both the forged and extruded alloys.

Keywords gigacycle fatigue; ultrasonic torsion testing system; continuous tests; titanium alloy; crack initiation.

NOMENCLATURE

HCF	= high cycle fatigue
SEM	= scanning electron microscope
UTS	= ultimate tensile strength
VHCF	= very high cycle fatigue
x	= spatial coordinate
t	= time
ρ	= volumetric mass
G	= dynamic shear modulus
$\mathcal{J}_p$	= polar moment of inertia
$\mathcal{J}_T$	= torsion stiffness
φ	= twist angle
$S(x)$	= cross section area at x
E	= Young modulus
σ_Y	= yield stress
ε_R	= deformation at rupture

INTRODUCTION

The in-service loads applied to real components are generally multiaxial and combine different loading modes, such as tension–compression, tension–tension, bending and torsion. For example, the in-service loading mode of train wheel axles is rotating–bending. Turbine rotor components are often subjected to static loads because of centrifugal force and additional bending and/or torsion loads because of vibrations induced via the gas or steam flow. In case of modern applications the loading frequencies are varying in a wide range from several

Correspondence: T. Palin-Luc. E-mail: thierry.palin-luc@ensam.eu

Hertz up to several kilo-Hertz. This leads to the accumulation of a very high number of loading cycles (typically 10^8–10^{10}) during the components life.[1]

As shown by Japanese researchers[2,3] in mid-1980s, structural materials can fail at greater than 10^7 cycles. Soon after, Bathias and co-workers experimentally established the concept of gigacycle fatigue failure.[4] Thus, investigating the fatigue behavior of structural materials beyond 10^7 cycles has become an important subject to ensure the long-term safety of real structures.[5] Using conventional fatigue testing techniques such as: servo-hydraulic, electro-dynamic or electromagnetic testing machines is not appropriate for the Very High Cycle Fatigue (VHCF) regime, because the testing time needed to apply 10^9 or 10^{10} cycles is too long (1157 days at 100 Hz for 10^{10} cycles, but less than 6 days at 20 kHz). Thus, investigating fatigue strength properties in the VHCF region requires the use of accelerated testing methods, such as ultrasonic fatigue testing systems.[6] Since the beginning of the 1990s several laboratories over the world have started developing ultrasonic fatigue testing devices and methods.[7–10] Early ultrasonic fatigue testing machines performed only uniaxial constant amplitude fatigue tests, with an R-ratio of -1, and were designed based on the Mason piezoelectric machine.[11] This type of machine did not find widespread use because of difficulties concerning the control of the ultrasonic fatigue testing system at that time. With progress in computer technologies it became possible to precisely control the loading parameters at high frequencies.

The first ultrasonic fatigue testing machine with a high-performance computer control system was developed by Bathias and co-workers[12] in the late 1980s. This testing system with a high-performance feedback loop allowed continuous servo-control of the loading parameters. Computer servo-controlling was an important step in the development of ultrasonic testing methods, and combined with a specimen air cooling system it made it possible to carry out continuous (as opposed to interrupted) ultrasonic fatigue tests.[1] Ultrasonic fatigue testing machines without high-performance computer control and cooling systems are operating in the pulse-pause regime.[13] Thus, further progress in ultrasonic fatigue testing techniques was developed in two different ways: continuous and pulse-pause loading.

Different loading conditions for real components have required the development of ultrasonic fatigue testing systems capable of applying loading modes such as: fully reversed tension, tension–tension, bending, fretting fatigue and torsion.[14] Some of these ultrasonic fatigue testing machines have already been commercialized (such as the tension–compression systems). Others are still under development (torsion). This paper is focused on a new torsion testing system.

In the following section a brief literature review of ultrasonic testing machines is presented. Then, the concept of ultrasonic torsion fatigue test is presented together with rotational elastic wave theory and the methodology used to design the new piezoelectric torsion machine. This system has been used for the first time to investigate the VHCF properties of the aeronautical titanium alloy VT3-1 (similar to Ti–6Al–4Mo) produced by forging or by extrusion. The testing conditions and the fatigue test results are presented, followed by optical and scanning electron microscope (SEM) observations of the fracture surfaces. Finally a discussion of the crack initiation mechanisms in pure shear is presented. It is seen that these depend on the manufacturing process (forging or extrusion).

LITERATURE REVIEW OF ULTRASONIC FATIGUE TESTING MACHINES

There are two types of ultrasonic torsion fatigue testing machines: (i) direct and (ii) indirect. The first one is based on a longitudinal-torsion piezoelectric converter. The second one (i.e. indirect machine) is based on an axial tension–compression piezoelectric converter. The longitudinal-torsion piezoelectric converter is made from piezoelectric motors, designed by Ueha and Ohya in Japan[15] and is also used by Mayer.[16] They transform a sinusoidal electrical signal into angular torsional vibrations. Ueha and Ohya helped Mayer to use this direct torsion system to study the VHCF behavior of high-strength aluminum alloy[13] in pure shear. These tests were performed under pulse-pause torsion loads with a pause duration of 50 to 1000 μm, to allow the specimen to cool. The results for this aluminum alloy show that this material can fail at greater than 10^7 cycles under pure torsion. The fatigue failure surfaces have a 'saw tooth' shape or a 'factory roof' type topography that is similar to observations in the HCF regime with tests at lower frequency. Despite this qualitative agreement between the ultrasonic fatigue test results and the results under conventional testing conditions, the determination of the total fatigue life is uncertain. Indeed, because of the pulse-pause technique the loading condition is close to being variable amplitude, requiring the use of a fatigue damage accumulation concept. Furthermore, the total number of applied cycles is questionable. Do the cycles at the beginning of a pulse, when the amplitude is being ramped up to the command value contribute to the final damage and the fatigue life? The same question is valid for the cycles at the end of a pulse when the amplitude is being ramped down.

This problem is common to all ultrasonic testing systems operating with the pulse-pause technique, and is the

reason why a torsion piezoelectric system, working in the continuous regime, has been designed by Bathias and co-workers.[17] This testing system is an 'indirect' machine based on a tension–compression (or longitudinal) piezoelectric converter. A special system consisting of two perpendicular ultrasonic horns, transforms axial vibration into angular vibration (Fig. 1). This ultrasonic torsion machine is controlled by a high performance computer and includes an air-cooling system that allows continuous constant amplitude torsion tests to be carried out. Despite the improvement in the operating mode via continuous loading, this system of ultrasonic horns has an Achilles heel. The connecting component (i.e. the pin in Fig. 1b) is subject to ultrasonic bending, resulting in a limited in-service lifetime. This implies that the pin needs to be changed after approximately 10^{10} cycles. Consequently, the lack of an ultrasonic torsion fatigue testing machine operating continuously with an appropriate in-service life is the motivation for this work and the development of a new piezoelectric torsion machine. Furthermore, because the system shown in Fig. 1 is not fully axial, the loads applied on the specimen are not pure torsional, there is a small secondary bending component.

ULTRASONIC TORSION FATIGUE TESTING CONCEPT

The ultrasonic torsion fatigue testing concept is similar to the axial tension–compression one. The ultrasonic fatigue testing frequency ranges from 15 kHz to 30 kHz with a typical frequency[1] of 20 kHz. The specimen is excited in resonance by an ultrasonic vibration at one of its natural Eigen modes. For the torsional case the ultrasonic vibration is angular (or rotational) and the resonance frequency corresponds to the first mode of torsion. All the mechanical parts of the ultrasonic fatigue testing system, including the specimen, are designed to be in resonance at the same loading frequency.

The servo-control concept applied to the ultrasonic torsion fatigue testing device is also quite similar that used for a tension–compression machine. All loading parameters are determined and continuously servo-controlled via dedicated software developed by the authors. The angular vibrations are generated by a direct piezoelectric torsion converter. This device transforms the ultrasonic sinusoidal electrical signal into mechanical angular vibrations at the same frequency. These vibrations induce a stationary elastic wave within the mechanical components of the machine (i.e. the horn and the specimen).

Rotational elastic waves and resonance frequency

The solution for the differential equations of motion for a three-dimensional infinite homogeneous isotropic elastic body shows that two types of elastic waves may exist: longitudinal and transverse. The ultrasonic torsion method is based on the theory of transverse wave propagation. For the case of a cylindrical bar in torsion, where the x-direction corresponds to its longitudinal axis, the equation of motion can be written as follows assuming a one dimensional problem[16] in the x-direction:

$$\rho \cdot \mathcal{J}_p(x) \frac{\partial^2 \varphi(x,t)}{\partial t^2} = G \frac{\partial}{\partial x}\left(\mathcal{J}_T(x) \frac{\partial \varphi(x,t)}{\partial x}\right) \quad (1)$$

where $\mathcal{J}_p(x)$ is the polar moment of inertia, $\mathcal{J}_T(x)$ is the torsion stiffness and $\phi(x)$ is the angular displacement.

Based on Equation (1) an analytical solution for all the mechanical parts of the ultrasonic torsion testing system can be derived. As usual the load applying part of the torsion machine consists of one or more ultrasonic horns, with constant cylindrical sections and with reduced cross section along the horn axis. Generally it is assumed that

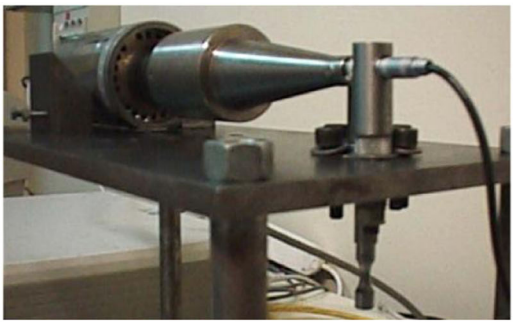

-a-

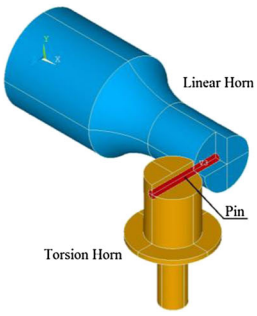

-b-

Fig. 1 a) Torsion testing machine with an axial piezoelectric converter;[14] b) scheme of the connection between the two perpendicular horns showing the pin.

increasing the size of the connection elements or connection surfaces increases the elastic wave energy dissipation because the contact between the different mechanical elements is not perfect. Thus, it is better to minimize the number of ultrasonic horns used in the design of a fatigue testing machine.

The proposed ultrasonic torsion fatigue testing system uses a single horn. It is directly connected to a piezoelectric converter (Fig. 2). The analytical solution for the elastic wave motion in such a horn may be determined by 'cross linking' the analytical solutions for the different parts labeled in Fig. 2: part (1) is a cylindrical bar with length L_1 and constant radius R_1 (20 mm in Fig. 1); part (2) has a reducing cross section along the axis of the horn; part (3) is similar to part (1) in that it is a cylindrical bar but with a smaller radius R_3.

Because all three parts of the ultrasonic torsion horn have axial symmetry in the x-direction, their polar moments of inertia are equal to their torsion stiffness $\mathcal{J}_p(x) = \mathcal{J}_T(x) = \frac{S^2(x)}{2\pi}$, where $S(x)$ is the cross-sectional area at distance x. Substituting the moment of inertial and the torsion strength into Equation (1) gives:

$$\frac{\partial^2\varphi(x,t)}{\partial t^2} - \frac{G}{\rho}\frac{1}{S^2(x)}\frac{\partial}{\partial x}S^2(x)\frac{\partial\varphi(x,t)}{\partial x} - \frac{G}{\rho}\frac{\partial^2\varphi(x,t)}{\partial x^2} = 0. \quad (2)$$

The general solution for the stationary wave in parts 1 to 3 of the ultrasonic horn (Fig. 2) can be found in the following form:

$$\text{Part N° 1}: \ \xi_1(x) = C_1 Sin(\omega t) + C_2 Cos(\omega t) \quad (3a)$$

$$\text{Part N° 2}: \ \xi_2(x) = \frac{C_3 e^{\beta\cdot x} + C_4 e^{-\beta\cdot x}}{\cosh(\alpha(L_1 + L_2 - x))} \quad (3b)$$

$$\text{Part N° 2}: \ \xi_3(x) = C_5 Sin(\omega t) + C_6 Cos(\omega t) \quad (3c)$$

where $\xi(x)$ is the time independent part in the time function $\varphi(x,t) = \xi(x)\cdot e^{i\omega t}$. Constants C_i in Equations (3a), (3b) and (3c) can be found by satisfying the following boundary conditions:

$$\text{At } x = 0: \begin{array}{l} \xi(x)|_{x=0} = \xi_0 \\ \xi'(x)|_{x=0} = 0 \end{array}; \quad (4a)$$

$$\text{at } x = L_1: \begin{array}{l} \xi_1(x)|_{x=L_1} = \xi_2(x)|_{x=L_1} \\ \xi_1'(x)|_{x=L_1} = \xi_2'(x)|x = L_1 \end{array}$$

$$\text{At } x = L_1 + L_2: \begin{array}{l} \xi_2(x)|_{x=L_1+L_2} = \xi_3(x)|_{x=L_1+L_2} \\ \xi_2'(x)|_{x=L_1+L_2} = \xi_3'(x)|_{x=L_1+L_2} \end{array} \quad (4b)$$

$$\text{at } x = L_1 + L_2 + L_3: \ \xi_3'(x)|_{x=L_1+L_2+L_3} = 0.$$

Design of a new ultrasonic torsion testing system

The design of the ultrasonic torsion fatigue testing system has been done in two steps. First, an analytical approach was used to pre-dimension the horn geometry. Second, finite element analyses were done to optimize the geometry. In the first step the following key dimensions of the horn (Fig. 2) were computed: L_1, L_2 and the resonance length L_3. As per all the ultrasonic horns designed by Bathias and co-workers, the length of the head part is made equal to one fourth of the stationary wavelength, independently of the excitation mode. The length of the tapered part (L_2) is calculated based on simple geometric considerations in order to reduce the stress concentration effect because of the decrease in diameter. The resonance length, L_3, is calculated based on the analytical solution given by Equations (3) and (4). This resonance length is a function of all the dimensional parameters (L_1, L_2, R_1, R_2 and constants of the hyperbolic profile) and of the elastic properties of the material (dynamic modulus, density and Poisson ratio).

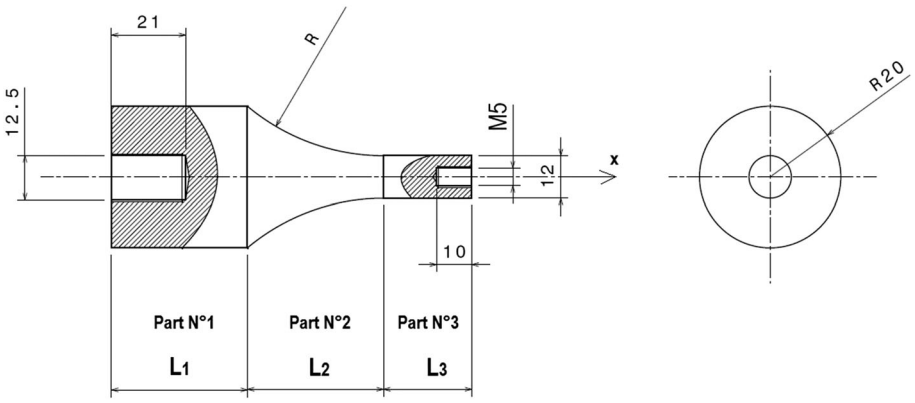

Fig. 2 Geometry of an ultrasonic torsion fatigue testing horn (dimensions in mm).

For the second step the dimensions of the horn are optimized in order to obtain a natural frequency close to the required value (of 20 kHz in the present case). Furthermore, as the amplitude of angular displacement produced by the piezoelectric converter does not exceed several mRad it has to be amplified by adjusting the diameters of the head and resonant parts. At the same time the cyclic stress generated during a fatigue test at the cross section $x = L_1 + L_2$ (Fig. 2) should be significantly lower than the fatigue strength of the material used to make the horn. Consequently, during the optimization process some corrections to the tapered section geometry can be made in order to decrease the stress concentration effect. A compromise has to be achieved in terms of the following two important points: (i) to obtain a magnification factor that is high enough (i.e. the ratio between the amplitude of vibration at the end of the horn to the amplitude applied at the top of it) and (ii) to reduce the stress in stress concentration zones (i.e. zones where the diameter changes, at $x = L_1 + L_2$).

The design of the torsion ultrasonic specimen (Fig. 5) is done following the same procedure outlined above for the horn. The diameter of the cylindrical part with constant cross section is chosen to be equal to 10 mm to allow the space for the M5 screw. The smallest diameter in the working section can vary from 4 to 5 mm. Nevertheless, the most common diameter for ultrasonic torsion specimens is 4 mm. After fixing the working section, the resonance length of the specimen can be adjusted so that the specimen has the required natural frequency of 20 kHz in torsion. As per the horn design, after the determining the key dimensions by analytical analysis, an additional numerical optimization has been carried out by finite element analysis.

EXPERIMENTAL EQUIPMENT AND INVESTIGATED MATERIALS

Ultrasonic torsion fatigue testing system

The ultrasonic torsion fatigue testing system used in this work uses a direct piezoelectric torsional transducer (in rotation) manufactured by the BRANSON Company in order to avoid the drawback of using two perpendicular horns and the failure of their connecting pin (see Fig. 1). A piezoelectric converter is driven by a high frequency electric sinusoidal signal with an amplitude in the range of 0 to 10 V. This piezoelectric transducer can achieve a maximum twist angle of 0.25 mRad for an amplitude of 10 V. In order to control the loading parameters (i.e. the amplitude of the twist angle and the loading frequency) and to count the number of loading cycles, a computer equipped with a high speed data acquisition and control card and dedicated control software was employed. The basic principal of the torsion ultrasonic testing machine is similar to a continuous (no pulse-pause) tension–compression system. The ultrasonic torsion fatigue testing system is illustrated in Fig. 3. The cooling system, consisting of compressed air delivered via an air gun, allows continuous fully reversed torsion fatigue tests to be carried out at temperatures close to room temperature.

The calibration of the torsion testing system was carried out using the strain-gauge technique (with AE10 glue from the Vishay Micro-measurement Company). A wide band (0–100 kHz) strain gauge conditioning device (2210 type Vishay Micro-measurement Company) was used. This equipment was also used by Perez-Mora *et al.* to calibrate ultrasonic fatigue tests in tension–compression.[18] The calibration data shows a linear relationship between the voltage of the control signal applied to the piezoelectric converter and the measured strain amplitude, which can be

-a- -b-

Fig. 3 a) The new ultrasonic torsion testing system; b) zoom on the transducer, the horn and the specimen.

Table 1 Chemical composition of VT3-1 titanium alloy (weight %)

Russian standard										
Fe	C	Si	Cr	Mo	N	Al	Zr	O	H	Ti
0.2–0.7	<0.1	0.15–0.4	0.8–2	2–3	<0.05	5.5–7	<0.5	<0.15	<0.015	Balance
Forged alloy										
Fe	C	Si	Cr	Mo	N	Al	Zr	O	H	Ti
0.7	—	0.29	2.1	2.1	—	6.1	—	—	—	Balance
Extruded alloy										
Fe	C	Si	Cr	Mo	N	Al	Zr	O	H	Ti
0.46	—	0.32	1.25	2	—	6.3	—	—	—	Balance

recalculated into an elastic stress amplitude. Furthermore, the strain measurement during ultrasonic torsion fatigue tests shows that the strain amplitude is stable during a fatigue test with an accuracy of +/−3%, except at the end of the test during a few seconds when the fatigue crack propagates.

Materials and specimens

For the initial tests using this new ultrasonic torsional fatigue testing machine an aeronautical titanium alloy has been chosen. The VT3-1 (similar to Ti–6Al–4Mo) Russian titanium alloy used to manufacture turbo-jet engine components was investigated.[19] This alpha beta titanium alloy was produced by two different techniques: forging and extrusion. The chemical composition of these materials (forged and extruded) is in agreement with the Russian state standard[20] (see Table 1).

The mechanical properties under monotonic quasi-static loading at room temperature are listed in Table 2, where E is the Young modulus, σ_Y is the yield stress, ε_R is the deformation at rupture and UTS is the ultimate tensile strength. The deformation at rupture for the extruded alloy is twice that of the forged alloy, and as expected, the forged alloy is less ductile than the extruded one.

Table 2 Mechanical properties of forged and extruded VT3-1 titanium alloy

Process	E (GPa)	σ_Y (MPa)	ε_R (%)	*UTS* (MPa)
Forging	116	930	6	980
Extrusion	110	1030	12.5	1100

The microstructure of extruded and forged VT3-1 titanium alloy is illustrated in Fig. 4. The microstructure of forged titanium alloy (Fig. 4a) consists of elongated alpha-platelets which are grouped in clusters of similarly orientated grains which are referred to as 'macrozones'.[21,22] The dominate orientation of alpha-platelets within two neighboring 'macrozones' is not always the same, as well as the morphology (shape) of the grains. Sometimes, fine lamellar alpha-platelets can be found within a 'macrozone', sometimes rough quasi-globular alpha-platelets. The microstructure of extruded titanium alloy is more homogeneous except in zones located in the center of the extruded bar. In the center of the bar, the microstructure is composed of alpha-phase needles formed within the primary beta-phase grains. The thickness of these needle structures is several tenths of micrometers, while their length can reach 15–20 μm. Outside of the center zone of the extruded bar, the microstructure consists of fine globules with a characteristic diameter of about 2 μm. The microstructure of the extruded titanium alloy changes from the center to the lateral surface of the bar via gradual refinement of the globules. To quantify possible heterogeneity in the mechanical properties of the alloys, Vickers

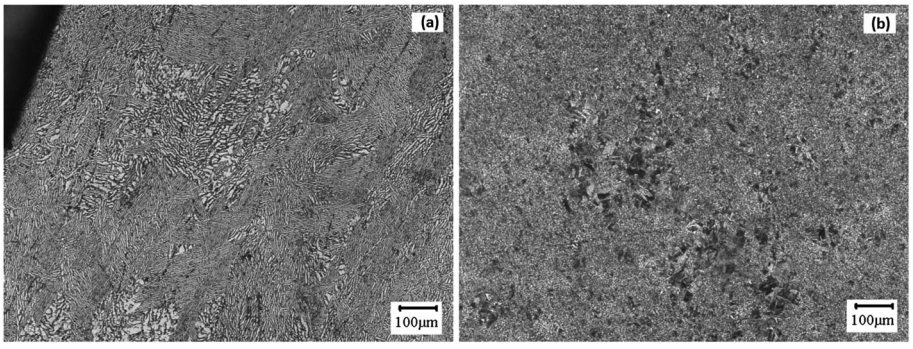

Fig. 4 Microstructure of (a) forged VT3-1 and (b) extruded VT3-1 titanium alloy.

micro-hardness (500 g) was carried out. The results are detailed in Ref. [21] Despite the microstructural heterogeneity of the extruded bars, as previously described, the micro-hardness of the extruded titanium alloy is more homogeneous than the forged one. The average values of micro-hardness for VT3-1 are similar: 366 HV for forged VT3-1 and 373 HV for the extruded alloy.

The specimens made from the forged titanium alloy were machined in the rim part a real turbo-jet engine compressor disks. The longitudinal axis of these samples was perpendicular to the plane of the plateau part of the disk. The specimens made from the extruded alloy were machined from bars with an external diameter of 14 mm. The longitudinal axis of the specimens is orientated along the direction of extrusion. As explained in the previous section, all the specimens for ultrasonic torsion tests were designed to be in resonance at the natural frequency of the complete ultrasonic testing machine (20 kHz). The specimen geometry is shown in Fig. 5.

RESULTS AND DISCUSSION

Fatigue test results

Fatigue tests were conducted until failure of the specimen or until a fatigue life of 10^9 cycles has been achieved. The results are plotted in Fig. 6. This figure shows that fatigue failure can occur at greater than 10^6 cycles, for both materials. As observed in fully reversed tensile fatigue tests for many other materials (steels and aluminum alloys)[1] the data for the forged titanium alloy shows a strong tendency to decrease its fatigue strength with increasing numbers of cycles. This tendency is less marked for the extruded VT3-1 titanium alloy. Indeed, the scatter in the fatigue strength data for the extruded alloy is greater than for the forged one. Additional fatigue tests should be carried out to confirm this observation.

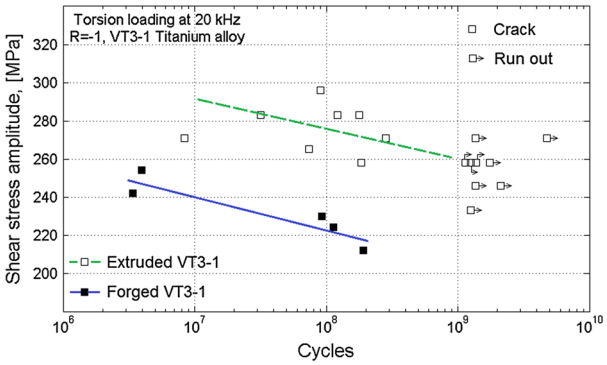

Fig. 6 Experimental fatigue test results in torsion (R= −1) at 20 kHz on smooth specimens in forged and extruded VT3-1 titanium alloy.

About the temperature

As previously discussed, all fatigue tests were carried out at room temperature (approximately 20 °C) with air cooling to ensure that the temperature of the specimen is not too elevated during the test and to avoid any parasitic effects because of self-heating. Infrared temperature measurements were carried out with a FLIR infrared camera (FLIR A300, spectral range 7.5 – 13 µm) during some fatigue tests (with air cooling). In order to neglect the effect of the emissivity of the specimen surface on the temperature measurements, the specimens were covered with a fine coat of mat black paint. The apparatus is illustrated in Fig. 7a. The evolution of the specimen temperature versus the shear stress amplitude is plotted in Fig. 7b. Even if the torsion fatigue tests were carried out under constant amplitude loads, without pulse-pause, these measurements show that specimen heating can be neglected for these materials in these testing conditions. Indeed the maximum increase in temperature is less than 10 °C (compared to room temperature).

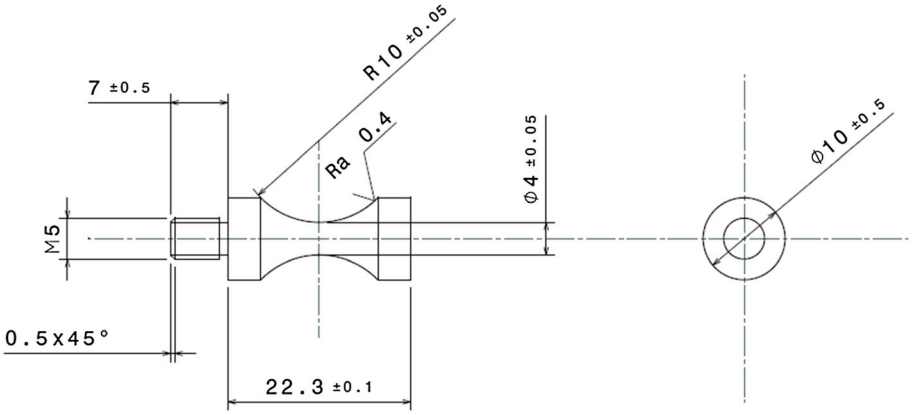

Fig. 5 Geometry of the specimen in VT3-1 titanium alloy for torsion fatigue test at 20 kHz.

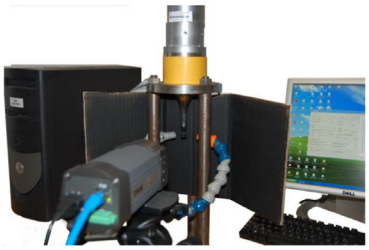

-a-

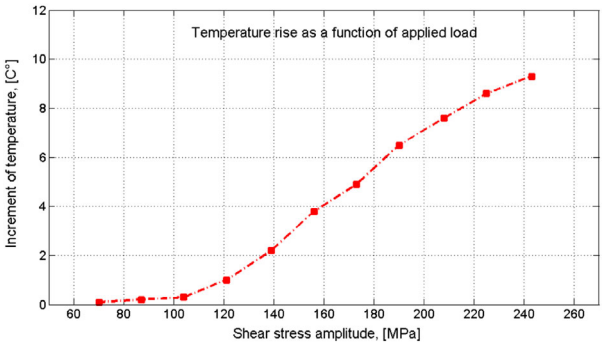

-b-

Fig. 7 a) Torsion testing machine with the infrared camera and b) temperature increase compared to room temperature in steady state regime versus the shear stress amplitude on forged titanium alloy.

Optical and SEM observations

The surfaces of all the tested specimens were observed with an optical binocular (Fig. 8). For all tested specimens, fatigue crack initiation in the gigacycle regime occurred in a plane perpendicular or parallel to the specimen axis. That is a plane of maximum shear stress amplitude. The fatigue cracks subsequently turned to propagate on a plane of maximum principal stress (at 45° to the longitudinal specimen direction). This result is very typical in the HCF regime and confirms that in VHCF cracks initiate in mode II (stage I) and bifurcate in mode I (stage II) when their length is greater than a few grains.[23]

Some torsion cracks branched onto two 45° planes on the specimen surface to form the classical X-type cracks during propagation or stage II (see Fig. 8a). Others have just one branch or one main torsion crack (see Fig. 8b). In both cases the specimen does not break into two halves, because of the high ductility of the titanium alloy. A special technique was developed to rupture the specimens with 45° torsion cracks so as to have access to the failure surface. First, wire electrical discharge machining was used to cut the non-broken part of the specimen, located at the opposite side of the crack. Then the specimen was immersed in liquid nitrogen and then broken open with a sharp impact.

SEM observations of the fracture surfaces show that the mechanisms of fatigue crack initiation and propagation are strongly dependent on the fabrication process. For the extruded titanium alloy, most of the time (but not always as shown later) crack initiation is located at the specimen surface. This is normal for torsion loads because the shear stress is maximum at the surface. Two zones of crack propagation can be easily identified on the fracture surface (Fig. 9). The first stage of crack propagation exhibits a relatively smooth surface without crack branching patterns (see Fig. 9a). The second zone is characterized by wing-like patterns which correspond to different torsion cracks growing at the same time in parallel planes inclined at 45° to the longitudinal axis.

The fracture surface is severely damaged near the crack initiation area because of the friction between the torsion crack surfaces. This makes it difficult to estimate the threshold length for torsion crack branching. Some fracture surfaces show elements of branching at a very early stage of cracking. Thus, it is probable that the absence of signs of crack branching on initiation zone of the fracture surface (within an elliptical zone with smaller half-diagonal of several hundreds of micrometers), can be explained by the destructive effect of crack surface fretting. Additionally, it should be noted that there are no flaws or defects in this material that are responsible for crack initiation. Thus the part of the crack in the

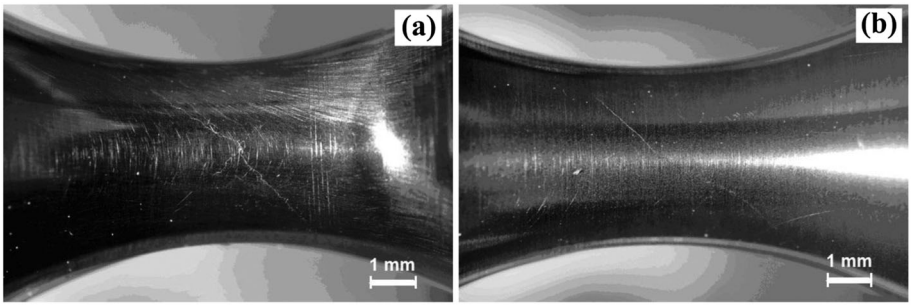

Fig. 8 (a) X-type crack after $N_f = 1.92 \times 10^8$ cycles under shear stress amplitude $\Delta\tau/2 = 212$ MPa and (b) single torsion cracks after $N_f = 1.84 \times 10^8$ cycles under $\Delta\tau/2 = 258$ MPa in VT3-1 titanium alloy ($R = -1$).

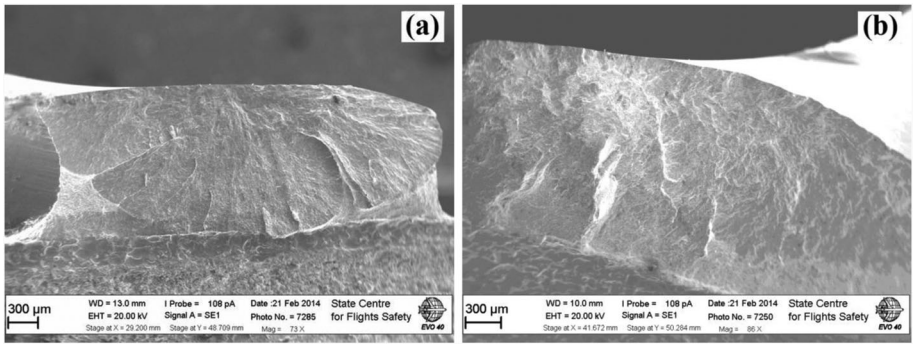

Fig. 9 Fracture surfaces of (a) extruded VT3-1 after $N_f = 1.84 \times 10^8$ cycles under $\Delta\tau/2 = 258$ MPa and (b) forged VT3-1 after $N_f = 1.13 \times 10^8$ cycles under $\Delta\tau/2 = 224$ MPa.

initiation zone and the branched cracks are the result of the local stress–strain state in the material.

For the forged titanium alloy, the fracture surface is more perturbed, as illustrated in Fig. 9b, with numerous secondary cracks near to the crack initiation site as well as far away. This fatigue cracking mechanism is typical for forged titanium alloys. Torsion crack branching is more intensive and some signs of this process can be found on the lateral surface of the specimen even close to the final crack length.

For both the extruded and forged titanium alloys crack initiation is not always located at the surface (see Fig. 10). However, because of numerous cracks in two perpendicular directions it is not easy to determine the position of main crack initiation or the first crack.

Figure 10a shows a crack initiation zone, in which internal crack propagation is interrupted by a second crack growing in a different 45° plane, perpendicular to the plane of the figure. This makes it possible to assume that the crack in the plane of the picture was initiated first. Internal crack initiation is not related to the presence of non-metallic inclusions. It is therefore likely to be associated with some defects-like features of the

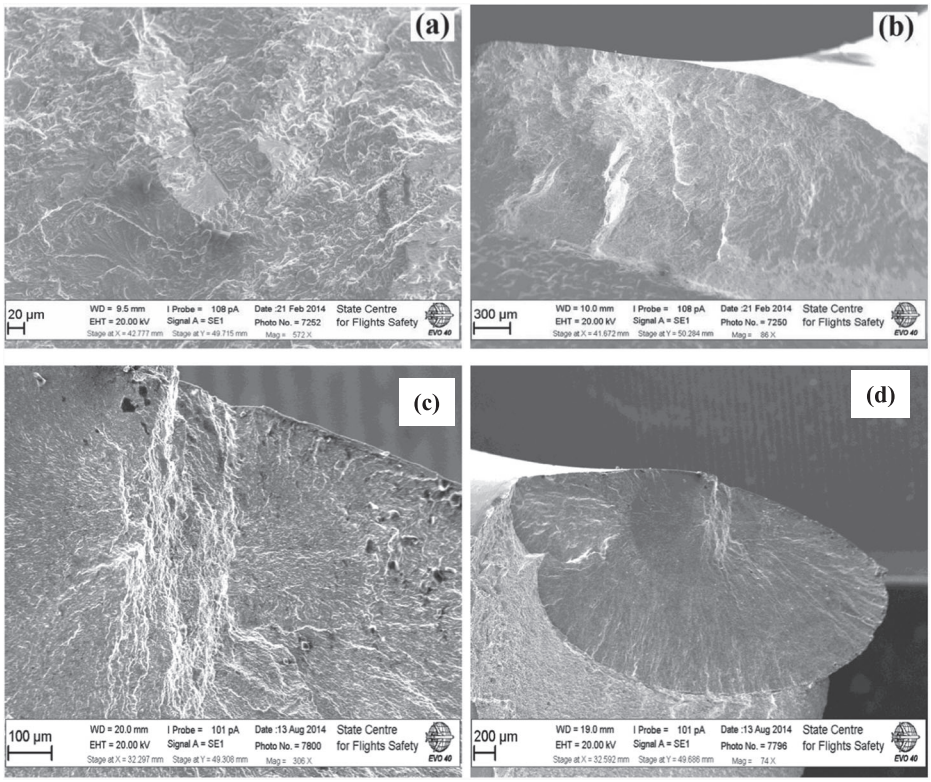

Fig. 10 Internal crack initiation and branching of torsion cracks, a and b) on the same forged specimen in VT3-1 titanium alloy under $\Delta\tau/2 = 224$ MPa, $Nf = 1.13 \times 10^8$ cycles, and c) and d) on the same extruded specimen in VT3-1 titanium alloy under $\Delta\tau/2 = 276$ MPa, $Nf = 1.67 \times 10^9$ cycles.

microstructure. The difference between the fatigue strength determined for the two materials is probably related to the difference in the internal matrix of the forged and extruded materials because they have different microstructures. Despite strong perturbations in the fracture surface roughness, some wings-like patterns have also been observed far from the crack initiation site. Hence in this case the torsion fatigue crack, in the forged alloy, is also growing in parallel planes, which are orientated at 45° to the longitudinal axis of the specimen (i.e. planes of maximum normal stress). For the extruded titanium alloy, internal cracking is very clearly seen in Figs 10c and 10d. This type of crack is referred to as a 'fish-eye' crack and is often discussed in the literature in the VHCF regime under tensile loads. However in this case no inclusion or defect is visible at the center of the fish-eye. Additional investigations and work should to be carried out to study how the fatigue properties of the two materials are influenced by the microstructure and the manufacturing process (i.e. forging and extrusion).

CONCLUSION AND PROSPECTS

Given the results presented in this paper, the following conclusions can be made:

(1) A new ultrasonic fatigue testing machine has been developed for continuous pure torsion fatigue tests ($R = -1$). The first VHCF tests results have been obtained for both forged and extruded VT3-1 aeronautical titanium alloys (similar to Ti–6Al–4V). Only these two materials have been investigated to date because this is a new fatigue testing system, other studies will be done in the near future.
(2) The fully reversed torsional fatigue resistance is higher for the extruded titanium alloy compared to the forged one.
(3) For crack initiation from the surface, the initial crack is located in planes experiencing the maximum shear stress amplitude, as per the HCF regime.
(4) For the extruded titanium alloy the fracture pattern was less perturbated compared to the forged alloy.
(5) For the two VT3-1 titanium alloys (forged and extruded) crack initiation was not always observed on the specimen surface, despite the fact that the maximum shear stress is located at the specimen surface and no non-metallic inclusion were observed to be at the origin of the fish-eye cracks.
(6) A high degree of branching of fatigue torsion cracks was observed as for extruded titanium alloy, as well as for forged one. Far from the crack initiation site, fatigue cracks grow in mode I, like in the HCF regime.

Additional microstructural investigations should be carried out to try to understand the relationship between crack initiation and short crack propagation and the microstructural features of the titanium alloys. It is possible that the macro-zones play a key role for the forged alloy. This has been observed by the authors for fully reversed tension in the VHCF regime[21] and by Le Biavan *et al.* also in tension, but in the HCF regime.[22] However, such an analysis is very difficult to carry out because of the complex microstructure of this alpha beta titanium alloy and because of the high degree of roughness of the fracture surface after torsional fatigue loading. Further progress in the understanding and prediction of crack initiation in the VHCF regime for this material could be obtained from micromechanical modeling. Indeed, crack initiation at very low stress strain amplitudes seems to be governed by the shear stress and strain at the interface between the alpha and beta phases like in a composite material with a matrix and fiber reinforcement.

Acknowledgements

The authors are grateful to the State Centre for Flight Safety in Moscow for providing the titanium alloy investigated and address a special thank you to Prof. A. Shanyavskiy for the interesting discussions and SEM observations. The authors are also thankful too to everyone in the SCFS who prepared specimens for SEM observations.

REFERENCES

1 Bathias, C. and Paris, P. C. (2005) *Gigacycle Fatigue in Mechanical Practice*. Dekker, New-York.
2 Naito, T., Ueda, H. and Kikuchi, M. (1984) Fatigue behavior of carburized steel with internal oxides and nonmartensitic microstructure near the surface. *Metall. Trans.*, **15A**, 1431–1436.
3 Asami, K. and Sugiyama, Y. (1985) Fatigue strength of various surface hardened steels. *Heat Treatment Technol. Assoc.*, **25**, 147–150.
4 Bathias, C. and Ni, J. (1993) Determination of fatigue limit between 10^5 and 10^9 cycles using an ultrasonic fatigue device. *ASTM Int.*, **1211**, 141–152.
5 Sakai, T. (2009) Review and prospects for current studies on very high cycle fatigue of metallic materials for machine structural use. *J. Solid Mechanics and Mater. Eng.*, **3**, 425–439.
6 Marines, I., Bin, X. and Bathias, C. (2003) An understanding of very high cycle fatigue of metals. *Int. J. Fatigue*, **25**, 1101–1107.
7 Xiangan, K., Saanouni, K. and Bathias, C. (1991) On the fatigue at very high frequency—part I: theoretical and variational formulation. *J. Eng. Mater. Technol.*, **113**, 205–209.
8 Xiangan, K., Saanouni, K., Thanigaiyarasu, G. and Bathias, C. (1991) On the fatigue at very high frequency—part II:

application to some materials. *J. Eng. Mater. Technol.*, **113**, 210–214.
9 Willetz, L. E. (1980) Ultrasonic fatigue. *Int. Mater. Rev.*, **25**, 65–78.
10 Stanzl, S. (1986) Fatigue testing at ultrasonic frequencies. *J. Soc. Environ. Eng.*, **25**, 11–16.
11 Mason, W. P. (1950) *Piezoelectric Crystals and their Application in Ultrasonics*. Van Nostrand, New York.
12 Wu, T. (1992) Modélisation de la fissure en fatigue vibratoire à haut temperature. Application aux alliages à base de nickel. PhD thesis, Ecole Centrale de Paris, France.
13 Stanzl-Tschegg, S. E., Mayer, H. R. and Tschegg, E. K. (1993) High frequency method for torsion fatigue testing. *Ultrasonics*, **31**, 275–280.
14 Bathias, C. (2006) Piezoelectric fatigue testing machines and devices. *Int. J. Fatigue*, **28**, 1438–1445.
15 Ueha, S., Nagashima, H. and Masuda, M. (1987) Longitudinal-torsion composite transducer and its applications. *Jpn. J. Appl. Phys.*, **26**, 188.
16 Mayer, H. (2006) Ultrasonic torsion and tension–compression fatigue testing: measuring principles and investigations on 2024-T351 aluminium alloy. *Int. J. Fatigue*, **28**, 1446–1455.
17 Marines-Garcia, I., Douset, J. P. and Bathias, C. (2007) Development of a new device to perform torsional ultrasonic fatigue testing. *Int. J. Fatigue*, **29**, 2094–2101.
18 Perez-Mora, R., Palin-Luc, T., Bathias, C. and Paris, P. C. (2015) Very high cycle fatigue of a high strength steel under sea water corrosion: a strong corrosion and mechanical damage coupling. *Int. J. Fatigue*, **74**, 156–165.
19 Nikitin, A., Shanyavskiy, A., Palin-Luc, T. and Bathias, C. (2012) *Fatigue Behaviour of the Titanium Alloy Ti–6Al–4Mo in Bifurcation Area at 20 kHz, ECF19*. ESIS, Kazan, Russia.
20 Russian State Standard. (2001) GOST-19807-91 wrought titanium and titanium alloys. Last revision 23 june 2009.
21 Nikitin, A., Palin-Luc, T., Shanyavskiy, A. and Bathias, C. (2014) Influence of production process of T–6Al–4Mo titanium alloy on crack initiation mechanisms in VHCF regime, 6th Int. Conference on Very High Cycle Fatigue, VHCF6, October 15–18, Chengdu, China, 9p on CD-Rom.
22 LeBiavant, K., Pommier, S. and Prioul, C. (2002) Local texture and fatigue crack initiation in a Ti–6Al–4V titanium alloy. *Fatigue Fract. Eng. Mater. Struct.*, **25**, 527–545.
23 Miller, K. (1982) The short crack problem. *Fatigue Fract. Eng. Mater. Struct.*, **5**, 223–232.